Crystal reorientation and wear mechanisms in MoS_2 lubricating thin films investigated by TEM

J. Moser and F. Lévy
Institut de Physique Appliquée, Ecole Polytechnique Fédérale de Lausanne, CH-1015 Lausanne, Switzerland

MoS_2 thin films are sputter-deposited in different conditions in order to obtain well-defined microstructures. They are submitted to ball-on-disk wear tests at moderate loads (0.7 GPa). Cross sections of wear tracks are observed by transmission electron microscopy (TEM). Sliding induces the formation and the wear of a lubricating buffer layer between the film and the sliding ball. This buffer layer shows strong crystal reorientation, suggesting the presence of intergranular motion. Initially amorphous films crystallize during the sliding test. The film's intrinsic failure mechanisms appear to be more determinant for the sliding lifetime than the properties of the interface.

I. INTRODUCTION

MoS_2 sputtered coatings are in use for lubrication in space and vacuum technology. Film performance is usually related to adhesion and structural properties. Adhesion can be improved by chemical treatment of the substrate[1-4] and/or ion beam mixing.[5-7] Structure is determined by deposition parameters such as substrate temperature, Ar pressure, power density, atmosphere purity, ion beam irradiation, etc. A wide variety of textures and morphologies have been obtained by those means.[8-13]

The sliding process has been shown to induce crystal reorientation, transfer film formation, and in some cases crystallization.[14-16] Using electron diffraction and Auger profiling, Fayeulle *et al.*[16] were able to show that the transfer film consists of MoS_2 and of reaction products of MoS_2 with atmosphere and/or slider materials. In this paper, we report on the investigation of cross-sectional samples by transmission electron microscopy (TEM) with lattice plane resolution. The aim is to characterize the structure of worn films, including all nontransferred materials at its surface, with depth resolution. This method appears to give important information for the understanding of wear mechanisms in MoS_2 thin films, as well as for describing lubrication at the appropriate scale of a few tens of nanometers. We apply this technique to samples of three well-characterized structures, obtained by sputtering with different deposition parameters.

II. EXPERIMENTAL

MoS_2 thin films are deposited by RF-magnetron sputtering. The substrates are 0.5 mm thick Si[100] wafers and polished 440C steel disks. They are sputter-cleaned before deposition with 100 eV Ar^+ ions. The total ion dose is $2 \cdot 10^{17}$ cm^{-2}. The target is commercial, 99% pure MoS_2, hot-pressed from powder. The deposition parameters are residual pressure before deposition, 10^{-6} Pa; RF powder density, 10 W cm^{-2}; and distance between target and substrate, 95 mm. Ar pressure and substrate temperature values shown in Table I produce, respectively, standard (STD), low Ar pressure (LAR), and low substrate temperature (LT) films. Some of the LT films are annealed in the deposition chamber, under vacuum, at 600 °C for 2 h (LTA films).

Wear tests are performed on a CSEM ball-on-disk apparatus, with a 6 mm diameter steel ball and a 5 N load. The Hertzian contact model,[17] which was shown to be relevant in the case of MoS_2 lubricating films,[18] gives an average pressure of the order of 0.7 GPa. The rotation frequency is 4 Hz, and the sliding velocity varies between 0.12 and 0.28 ms^{-1}. The tests are performed at room temperature under dry air (relative humidity RH $<2\%$) and humid air (RH $\simeq 40\%$). Samples on steel substrates are tested until the sliding coefficient μ reaches 0.3. Samples on Si substrates are submitted to a preset number of revolutions before preparation for TEM observation. Cross sections for TEM observation are prepared by mechanical polishing, followed by ion milling. The samples are observed in a direction parallel to the interface and perpendicular to the sliding direction.

III. RESULTS

A. As-deposited films

The deposition parameters were chosen in order to produce films of well-defined microstructures (see Fig. 1 and Table I). STD films are clearly crystallized. The crystallites have their (002) basal crystal planes perpendicular to the substrate, except in the first 5–10 nm near the interface, where they are parallel to the substrate. This structure has been investigated in more detail elsewhere.[19,20] LT films are almost amorphous,

TABLE I. MoS$_2$ deposition parameters and microstructures for different types of films.

Type of films	Deposition parameters		Structural characteristics		
	P_{Ar} (Pa)	T_s (°C)	Structure	Orientation	Morphology
STD	3.0	300	Crystallized	(002) $\perp$ substrate[a]	Lamellar
LAR	0.4	300	Crystallized	(002) $\parallel$ substrate	Dense
LT	3.0	30	Quasi-amorphous	Random	Dense
LTA	3.0	30[b]	Crystallized	Random	Dense

[a]Except in the first 5–10 nm near the interface (see text).
[b]Annealed at 600 °C in vacuum for 2 h.

with a few randomly oriented small crystallites, whose thickness in the **c** direction does not exceed 2 nm. When annealed (LTA), they crystallize with still randomly oriented basal planes. LAR films are dense, with basal planes mainly oriented parallel to the substrate.

Chemical compositions have been measured using Rutherford Backscattering Spectroscopy (RBS) and are shown in Table II. The S/Mo stoichiometric ratio does not vary much as a function of the deposition parameters, except in the case of the LAR sample, which is sulfur deficient. The presence of oxygen is detected using a resonance at 3 MeV. Usually, specific structure related to C is not observed in RBS spectra; however, calculations performed with a composition including only Mo, S, and O overestimate the film signal. Variable and often important amounts of C are then introduced into the RBS calculation in order to fit the respective intensities of the film and substrate signals. This indirect way of measuring the C content is the cause of an important incertitude, which appears in the error estimates of Table II. X-ray diffraction, electron diffraction, and high-resolution TEM investigations give no evidence of crystalline phases including carbon. Therefore, carbon is apparently present as a substitutional, interstitial, or amorphous phase in the film. A typical spectrum corresponding to an STD sample is shown in Fig. 2. The low-energy edges of the S and Mo signals appear broader than the corresponding high-energy edges, which width is determined by the instrumental resolution. This effect, also visible on the high-energy edge of the substrate signal, is usually interpreted in terms of a diffused interface. This interpretation is not consistent with TEM images, which show a well-defined interface. It is more likely an effect of the lamellar film structure, due to which the film thickness is not constant over the surface. In the case of the LAR sample, the calculation underestimates the film signal (S and Mo) with respect to the substrate signal. This phenomenon, probably due to channeling in the substrate, has as a consequence that the C content cannot be estimated the same way as above. Consequently, the absence of a C concentration value in the table does not mean that the films are carbon-free, but accounts for the impossibility to detect C in this case.

B. Tribological behavior

The respective tribological performances of the different types of films were evaluated by ball-on-disk wear tests on samples deposited on steel substrates. For all samples, the friction coefficient is typically below 0.04 in dry air, whereas it reaches about 0.3 in humid air. For comparison between films of different thicknesses (between 0.4 μm and 1 μm), lifetime values are divided by film thickness and are given in revolutions per nanometer. The variation of the friction coefficient with increasing sliding time in dry air shows different regimes. First, a smooth behavior is observed, with a friction coefficient $\mu = 0.03 \pm 0.01$. It corresponds to a steady sliding regime. Then the friction coefficient increases and shows oscillations and/or peaks, before the film undergoes complete wear. For measuring purpose, we define the end of the steady sliding regime as the time at which the friction coefficient reaches 0.1. Complete wear is considered to be when the friction coefficient reaches 0.3. Typical sliding lifetimes for each type of films are shown in Fig. 3. It can be seen that standard films exhibit shorter lifetimes, whereas LAR, LT, and LTA films last significantly longer. For LAR films, the duration of the steady sliding regime with respect to the total lifetime is longer than for STD films.

The TEM observations performed on wear tracks are characterized by an important scattering of the results, due to the inhomogeneity of the wear track, the observable area being limited to a few microns along the interface. It is nevertheless possible to describe a chronology of events by comparison of the different observations.

The successive stages of wear of a crystalline, lamellar film (STD) are shown in cross sections of Fig. 4. Figure 4(a) shows the surface of the film in the absence of sliding. The lamellae are clearly visible. The first effect of sliding is shown in Fig. 4(b), where the same film was submitted to 1000 revolutions. In this transitory situation, the lamellar morphology is not affected, except in the top 30 nm, where the basal planes are reoriented in a direction parallel to the direction of sliding. After further sliding, the structure becomes typical of the sliding regime until complete wear of the film [Fig. 4(c)].
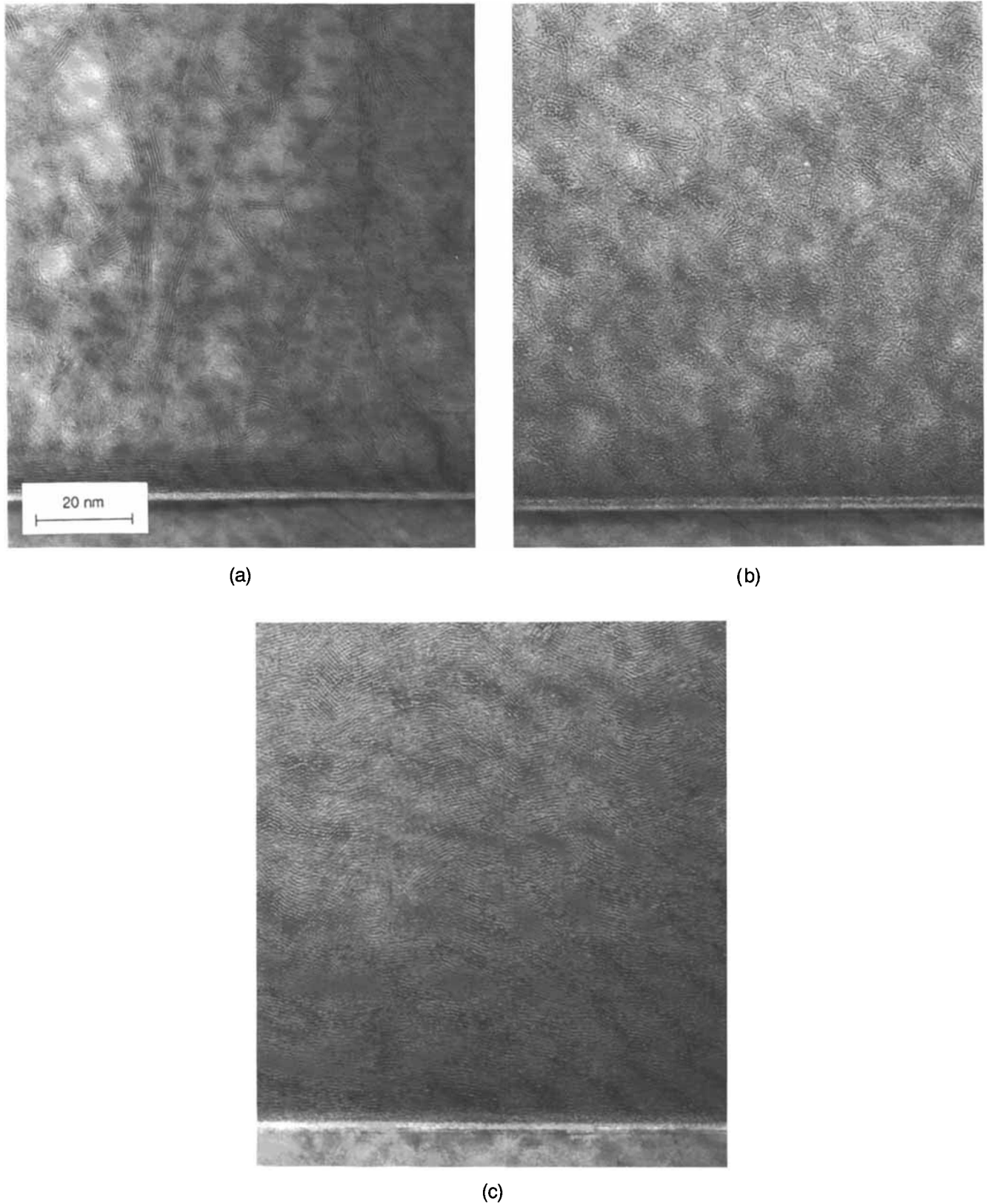
J. Mater. Res., Vol. 8, No. 1, Jan 1993

207

FIG. 1. As-deposited MoS$_2$ films on Si[100], cross-sectional TEM micrographs. The different structures correspond to different deposition parameters: (a) standard (STD); (b) room temperature (LT); (c) low argon pressure (LAR). The 1–2 nm amorphous layer between the film and the substrate is in (a) native silicon oxide, and in (b) and (c) silicon amorphisized by ion bombardment.

TABLE II. Chemical compositions measured by RBS.

Type of films	Atomic compositions		
	S/Mo	O/Mo	C/Mo
Standard (STD)	1.82 ± 0.05	0.1 ± 0.1	0.8 ± 0.2
Low Ar pressure (LAR)	1.47	0.05	...[a]
Low T_s (LT)	1.72	0.3	0.6

[a]See the text.

FIG. 3. MoS₂ thin films of different types (see text), normalized sliding lifetime for two different values of the friction coefficient μ: $\mu < 0.1$: steady sliding, $\mu < 0.3$: complete wear. Typical standard deviation: 50%.

Two zones are observed: (a) Near the film-substrate interface, the bulk of the film is roughly unaffected by the sliding and conserves its as-deposited structure. (b) Near the film surface, a buffer layer takes form and separates the bulk of the film from the sliding ball. This buffer layer is characterized by a strong densification and a reorientation of basal planes. The basal planes form a pattern of "flow lines", which corresponds to a decrease of the tilt angle between crystallites (angle between respective basal planes). On both sides of the interface between these two zones, the basal planes are nearly parallel to each other. The formation of a crack is often observed along this interface. The final step, observed after sample failure, is shown in Fig. 4(d). The film thickness is reduced to a few monolayers, with basal planes parallel to the interface. The originally single-crystalline Si substrate is amorphisized down to 50 nm below the interface, presumably due to cold-work induced by the very high stresses of the no-longer lubricated system.

Qualitatively, the LT and LAR films behave similarly, except for the following specificities: LT films subjected to sliding develop a buffer layer extending ultimately through the whole film except a 20 nm thick
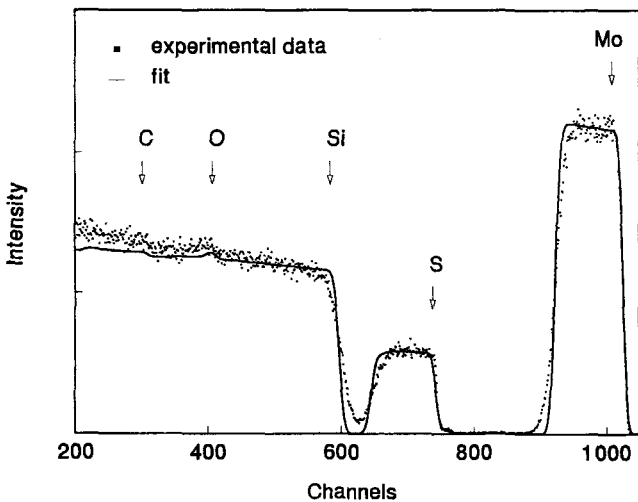

FIG. 2. RBS spectrum of an STD sample. Dots: experimental data; continuous line: fit produced by calculation from composition values in Table II.
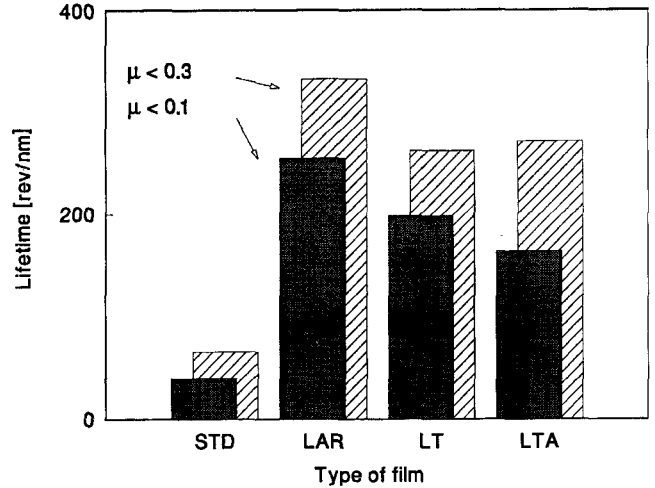
interfacial region. This buffer layer shows a well-defined pattern of basal planes, whereas the aspect of the interfacial region remains quasi-amorphous even shortly before the failure stage (Fig. 5). Although part of this feature can be explained by reorientation, its magnitude suggests that crystallization occurs during sliding, as observed, e.g., by Hilton[14] using x-ray diffraction measurements.

As-deposited LAR films originally are already partially oriented; they do not undergo a strong wear-induced reorientation. Nevertheless, a buffer layer can form, which has a different aspect than the bulk of the film (Fig. 6). It is more disordered, with a strongly reduced grain size in the c direction, sometimes down to one single molecular layer [one (002) fringe].

The observation of MoS₂ films submitted to sliding in humid air (40% RH) reveals the formation of cracks, a few nanometers away from the film-substrate interface. These cracks develop at an early stage, either when the buffer layer is still situated at the very surface of the film, or even in the absence of any buffer layer. This behavior can be explained by the higher stress in the film, due to the larger friction coefficient.

IV. DISCUSSION

Sliding on MoS₂ thin films appears to involve the formation of a buffer layer separating the bulk of the film from the sliding ball and the transfer film, as shown schematically in Fig. 7. This layer is indeed the active, lubricating part of the film. The "convective-like" or "turbulent-like" pattern formed by the basal planes suggests that mutual displacements of crystallites occur in this whole layer.
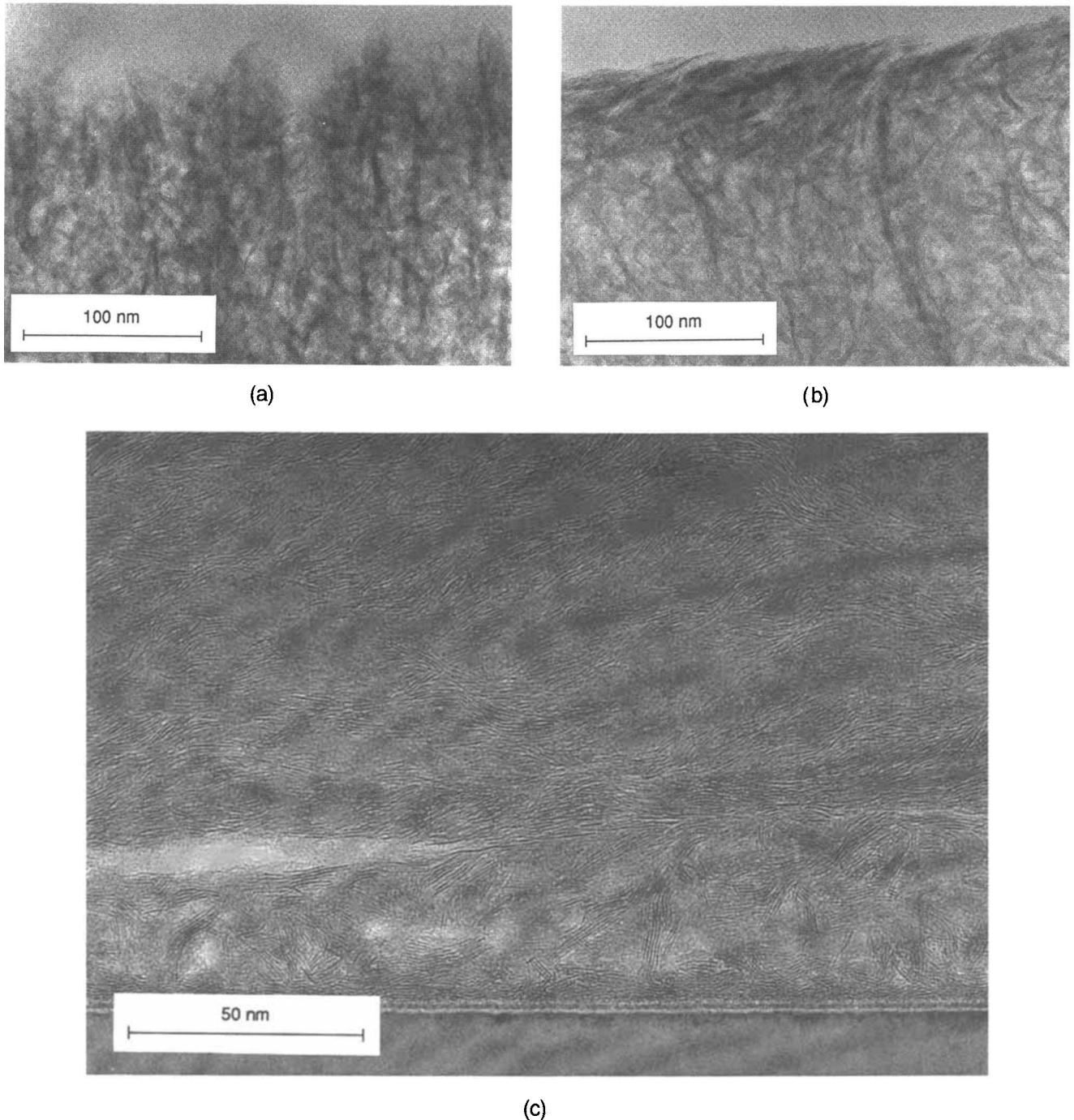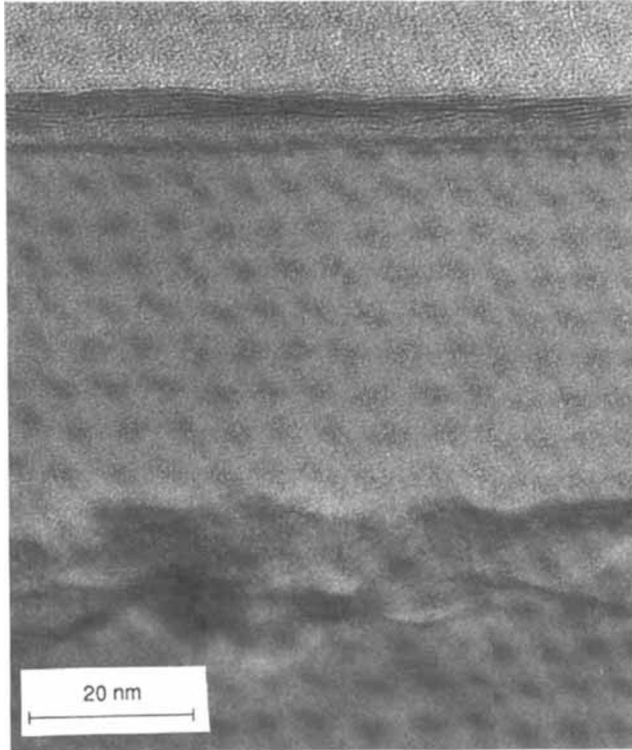
(a)

(b)

(c)

FIG. 4. MoS$_2$ films, cross-sectional TEM micrographs corresponding to different stages of wear: (a) unworn sample, (b) weakly worn sample (transitory regime), (c) medium worn sample (steady regime), and (d) severely worn sample.

According to Poirier,[21] plastic deformation of fine-grained materials can proceed by grain-boundary sliding. The voids created by the relative motion of grains are filled by atom and vacancy diffusion inside the grains at high temperature (diffusion creep). In our case, we consider grain-boundary sliding essentially along basal surfaces. The filling of voids and thus the high temperature condition are less necessary than in the general case for the following reasons. First, MoS$_2$ has a low adhesion between basal planes (easy cleavage). The creation of voids is energetically less expensive than in other materials. Second, the low tilt angles between basal surfaces in the buffer layer, leading to "flow line" patterns, provide sliding paths with only limited formation of voids.

The crystallization of quasi-amorphous (LT) films may also be related to intergranular motion. In the interfacial region, due to the presence of the substrate and

210

J. Mater. Res., Vol. 8, No. 1, Jan 1993

(d)

FIG. 4. (continued)

FIG. 5. Cross section of a worn semi-amorphous MoS_2 LT film.

FIG. 6. Cross section of a worn MoS_2 LAR film.

to the high density, the grains are tightly bound together and intergranular motion is difficult. This would explain why the interfacial region remains in its as-deposited quasi-amorphous state even near the failure stage. A mechanism can then be proposed for the wear process in MoS_2 films. It consists first in the tearing off of surface crystallites, forming debris, which are retained at the surface to form a reoriented buffer layer. This layer itself can be worn by two different mechanisms. The first one is the continuous erosion at the surface, releasing debris of the thickness of typically one single molecular layer (0.6 nm) [Fig. 8(a)]. In some cases, an amorphous, dark overlayer can be observed at the surface of the film, probably consisting also in worn material. The second mechanism consists in the tearing off of the whole buffer layer itself, following the formation of a crack at the interface between the lubricating and the unaffected part of the film. This situation, shown in Fig. 8(b), can lead to the loss of very important quantities of material. A crack occurs at an interface between domains with parallel orientation of the basal planes, forming a continuous plane along which the bonding between crystallites is specially weak. The cycle, consisting of the formation of the buffer layer and its subsequent wear, can be repeated until the total wear of the film is reached. In reality, these steps are probably partly simultaneous, and the process complicated by material transport along the track.
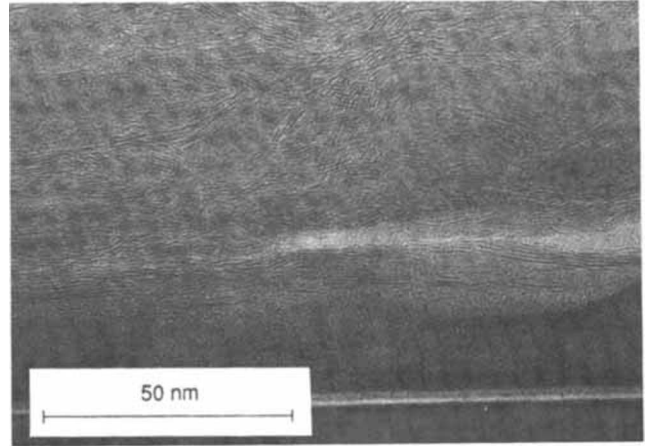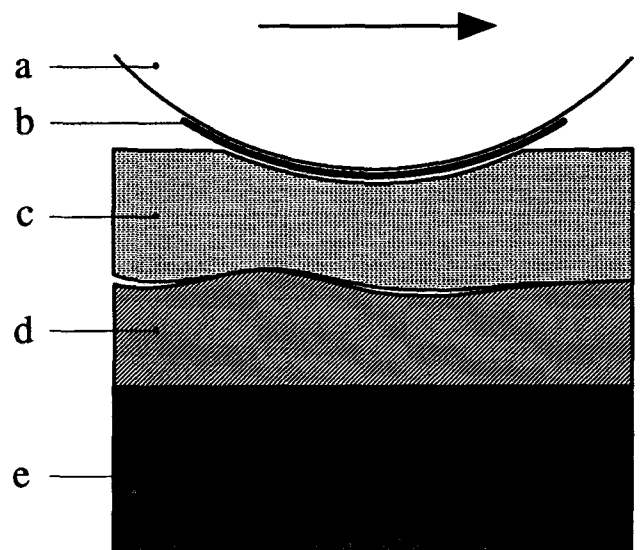

FIG. 7. MoS_2 film under sliding conditions: schematic cross section showing (a) the sliding ball, (b) the transfer film, (c) the lubricating buffer layer, (d) the bulk of the film, and (e) the substrate.
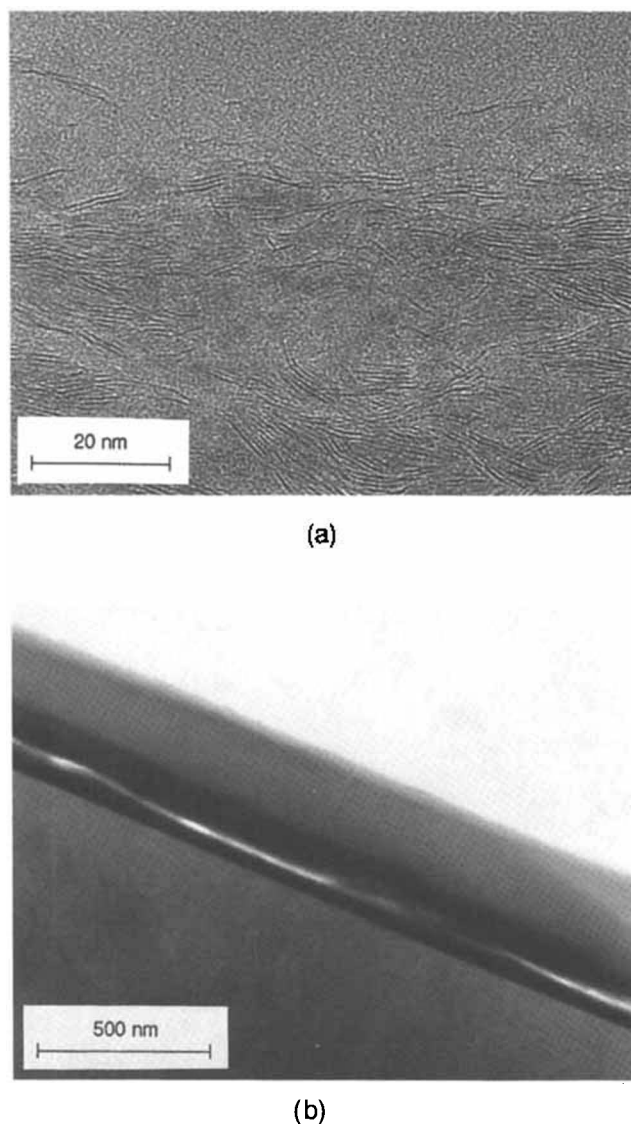
The reason why sliding induces an increase in grain size in the LT films, whereas we observe the opposite effect in the LAR films, is still unclear at the present stage of investigations. In particular, the degree of oxidation of the grains should be considered in the interpretation of buffer layer formation for both types of films.

V. CONCLUSION

Different kinds of MoS_2 films are sputter-deposited at various substrate temperatures and argon pressures. The resulting structures and morphologies can be quasi-amorphous or crystalline, with basal planes perpendicular to the interface (lamellar films) or parallel to it (non-lamellar films). In a ball-on-disk wear test, the higher performances are found for quasi-amorphous and for parallel-oriented films.

In all the films, effective lubrication is due to complex relative sliding motions between crystallites in a buffer layer separating the sliding ball from the lower, unaffected part of the film. The wear process can be described in terms of formation and wear of this buffer layer. In quasi-amorphous films deposited at room temperature, the sliding wear experiment initiates an increase of degree of crystallinity, which is likely due to a relative motion of crystallites in the film.

Finally, it appears that, at the medium loads used in our experiment, the adhesion of the film on the substrate is not as critical a cause of failure as the intrinsic properties of the film itself, since no peeling off of the film from the substrate was observed.

ACKNOWLEDGMENTS

REFERENCES

1. M. R. Hilton, R. Bauer, S. V. Didziulis, and P. D. Fleischauer, Thin Solid Films **201**, 49–58 (1991).
2. P. D. Fleischauer and R. Bauer, ASLE Trans. **30**, 160–166 (1987).
3. S. V. Didziulis and P. D. Fleischauer, Langmuir **6**, 621–627 (1990).
4. P. A. Bertrand, J. Mater. Res. **4**, 180–184 (1989).
5. N. J. Mikkelsen, J. Chevallier, G. Sørensen, and C. A. Straede, Appl. Phys. Lett. **52**, 1130–1132 (1988).

(a)

(b)

FIG. 8. Wear debris: (a) very small (approximately one molecular MoS₂ layer) debris at the film surface, and (b) big debris formed by the separation of the whole buffer layer.

In this context, the results from Fayeulle *et al.*[16] suggest two remarks. First, the debris released at the film surface are probably included in the transfer film covering the ball. Second, assuming that the transfer film consists of reacted materials (oxides), some of these reacted materials should be present in the buffer layer. They would diffuse from the surface by the intercrystalline motion and influence the lubricating properties. Nevertheless, whereas the above authors find crystalline oxides in their transfer films, we never observe any non-MoS_2 crystalline phase in our buffer layers. This indicates that oxygen should be present as substitutional or interstitial in the buffer layer, and confirms the different nature of the buffer layer on one hand, and of the transfer film on the other hand.

6. N. J. Mikkelsen and G. Sørensen, Mater. Sci. Eng. **A115**, 343–347 (1989).
7. R. S. Bhattacharya, A. K. Rai, and A. Erdemir, Nucl. Instrum. Methods in Phys. Res. **B59/60**, 788–792 (1991).
8. R. Bichsel, P. Buffat, and F. Lévy, J. Phys. D: Appl. Phys. **19**, 1575–1585 (1986).
9. V. Buck, Wear **114**, 263–274 (1987).
10. P. Gribi, Z. W. Sun, and F. Lévy, J. Phys. D: Appl. Phys. **22**, 238–240 (1989).
11. A. Aubert, J. Ph. Nabot, J. Ernoult, and Ph. Renaux, Surf. Coat. Technol. **41**, 127–134 (1990).
12. R. N. Bolster, I. L. Singer, J. C. Wegand, S. Fayeulle, and C. R. Gossett, Surf. Coat. Technol. **46**, 207–215 (1991).
13. C. Müller, C. Menoud, M. Maillat, and H. E. Hintermann, Surf. Coat. Technol. **36**, 351–359 (1988).
14. M. R. Hilton and P. D. Fleischauer, in *New Materials Approaches to Tribology: Theory and Applications,* edited by L. E. Pope, L. Fehrenbacher, and W. O. Winer (Mater. Res. Soc. Symp. Proc. **140**, Pittsburgh, PA, 1989), pp. 227–238.
15. M. R. Hilton, R. Bauer, and P. D. Fleischauer, Thin Solid Films **188**, 219–236 (1990).
16. S. Fayeulle, P. D. Ehni, and I. L. Singer, Mechanics of Coatings, Leeds-Lyon **16**, 129–137 (1990).
17. K. L. Johnson, *Contact Mechanics* (Cambridge University Press, 1985).
18. I. L. Singer, R. N. Bolster, J. Wegand, S. Fayeulle, and B. C. Stupp, Appl. Phys. Lett. **57**, 995–997 (1990).
19. J. Moser, H. Liao, and F. Lévy, J. Phys. D: Appl. Phys. **23**, 624–626 (1990).
20. J. Moser and F. Lévy, J. Mater. Res. **7**, 734–740 (1992).
21. J-P. Poirier, *Creep of Crystals* (Cambridge University Press, 1985).